EFFECTS OF MULTIPLE REDUCTIONS ON GRAIN REFINEMENT DURING HOT WORKING OF ALLOY 718

M. C. Mataya
Rockwell International Corporation
Golden, Colorado

D. K. Matlock
Advanced Steel Processing and Products Research Center
Colorado School of Mines
Golden, Colorado

Abstract

The simulation of microstructural evolution during primary breakdown of production sized alloy 718 ingots by radial forging was accomplished via multiple stroke axial compression testing of cylindrical specimens taken from a wrought and heat treated bar with a 254μm grain size. Four stroke compression test sequences were performed at a constant true strain rate of 1.0 s^{-1} and at temperatures of 950°C, 1050°C, and 1150°C. The applied strain per stroke for each four stroke sequence was either 0.14 or 0.23. Static, rather than dynamic, recrystallization was found to be responsible for the observed grain size refinement and its repetitive occurrence during back to back dwell periods resulted in the maintenance of a fine grain microstructure during multiple pass deformation sequences. In order of importance, the critical hot working parameters for recrystallization are temperature, dwell time between passes, and strain per pass. Microstructure was found to vary with work piece position, simulated by the applied sequence of dwell periods.

Superalloy 718—Metallurgy and Applications
Edited by E.A. Loria
The Minerals, Metals & Materials Society, 1989

Background

In lieu of the need for information regarding primary ingot breakdown of as-cast alloy 718, a research program was initiated at the University-Industry Advanced Steel Processing and Products Research Center at the Colorado School of Mines, Golden, Colorado, whereby the hot deformation behavior and microstructural response of production-sized ingot material would be characterized. Initially, two studies were designed and conducted in parallel to determine the effect of (a) ingot position for a constant set of hot working parameters [1] and (b) varying hot working parameters for a constant ingot position [2] on the dynamic stress-strain response and recrystallization behavior of as-cast alloy 718. It was shown in the first study [1] that variations in ingot structure, owing to positional differences, had a marked influence on flow stress, the shape of the stress-strain curve, and the deformed test sample geometry, however, recrystallization was independent of ingot structure and position. The results of the second study [2], summarized in a separate paper in this volume [3], demonstrated that grain size refinement occurs via static recrytallization.

These studies [1,2] were reviewed [4] in order to establish process design criteria for grain size refinement during primary breakdown of alloy 718 ingot via multiple pass radial forging. The discussion of that review, presented in part in the Introduction below, establishes the inadequacy of single pass deformation test data with regard to the prediction of microstructural evolution during passes subsequent to the first imposed during radial forging. This paper presents the findings from a follow-on study in which multiple-pass deformation sequences, simulating those of radial forging, were imposed on coarse grained alloy 718 test specimens and microstructural evolution was characterized.

Introduction

The need to fabricate complex shaped components having a fine uniform microstructure is a generic one and not limited to applications of alloy 718. The ability of the secondary processor to refine the structure existing in the starting material is limited because the work applied to preforms, often simple in shape, must be distributed non-uniformly to achieve a complex final shape. Consequently, the primary processor must often assume the responsibility for producing a fine uniform microstructure in intermediate size bar and plate and must therefore develop thermal mechanical-working techniques for the reduction of coarse inhomogeneous as-cast structures.

The desired reduction in grain size is achieved through recrystallization which may occur either statically or dynamically, implying the absence or presence of concurrent plastic deformation, respectively. In both cases, the stored energy of deformation, in the form of a dislocation substructure, is the driving force for recrystallization during which grain boundaries move to restore the worked volume to a relatively defect free state.

Recovery is a competitive softening process and occurs statically and dynamically. Recovery is characterized by the restoration of physical properties without a change in the grain structure through dislocation rearrangement and annihilation. Because these processes are enhanced by cross slip, metals with a high stacking fault energy, i.e. aluminum, exhibit recovery in preference to recrystallization. Due to composition, the stacking fault energy of alloy 718 is low to intermediate in value. Hence,

one would expect that both recrystallization as well as recovery would take place during thermal mechanical processing.

Production size alloy 718 ingots, are worked in a temperature range from 1150°C to 800°C. A typical large finished size may be 225mm (about 9 inches) in diameter. When processed via radial forging, work piece speed through the forging dies may be varied from 2 to 5m/min. The reduction in cross section area may be varied between 10 and 50 pct. with reductions of 15 to 20 pct. being more common. The strain-rate of deformation is approximately $1.0s^{-1}$.

With these typical parameters, a 2.5m long ingot traveling at 2.5m/min. through the inlet side of a radial forging machine would have a cycle time for the first complete pass of approximately one minute. During radial forging the ingot is worked in one direction through the die set with both the lead and tail ends passing completely through the dies to receive the full benefit of the applied reduction. The position of the work piece is then reversed so that the tail end, with respect to the first pass, is the first to be reduced during the second pass. A dwell time of 10 sec. is typical between material exit from the dies and reentry.

Figure 1 shows a schematic of the deformation dwell time history during radial forging for three different positions in an ingot (lead, midlength, and tail with respect to the first pass) for the initial four passes. As shown, after the lead end is deformed, one minute will elapse before the ingot exits the dies; one half minute will lapse for the midlength position before exit; and the tail end exits in zero time. Figures 12 and 13 from Weis et al. [3] show that for a deformation temperature of 1150°C the microstructure of the lead end would be about 70 pct. recrystallized after one pass, with a recrystallized grain size of 150μm, and 30 pct. worked and unrecrystallized. Correspondingly, the midlength would be 40 pct. recrystallized with a grain size of 80μm and 60 pct. worked, and the tail end would be 100 pct. unrecrystallized and worked. Similar predictions can be obtained for the second pass. Estimates of the microstructure as it evolves with time and with position along the length of the ingot are provided in Table I.

Finer structures at the midlength are predicted after the initial passes because there is less time for grain growth before the subsequent pass is applied (1 min. vs. 2 min. for the ends of the bar). Although coarser recrystallized grains are present in the lead end, a greater fraction of the volume is recrystallized due to the longer time, 2 min. vs. 1 min., between deformation impulses. Evolution of the microstructure during the later passes, however, is less predictable.

The purpose of this investigation was to characterize by simulation the evolution of microstructure during multipass radial forging of as-cast alloy 718. The simulation was accomplished by multiple stroke compression testing with applied strains and hold times between passes similar to those used in production.

Experimental Procedure

The alloy 718 material utilized in this investigation was cast, via vacuum induction melting followed by vacuum arc remelting, by the Carpenter Technology Corporation into a 406mm (16 inches) diameter cylindrical ingot. Subsequently, the ingot was homogenized in a conventional furnace to remove undesirable products of solidification, i.e. Laves phase, and to reduce microsegregation, especially titanium and niobium. The chemistry of the ingot is provided in Table II. The ingot was hot worked via radial forging

TABLE I - Prediction of Microstructure as a Function of Position and Pass for a One Minute Cycle Time Through A Radial Forge Machine at a Temperature of 1150°C, at a Strain-Rate of $1s^{-1}$ and for a Strain of 0.25. NOTE: UNREX Denotes Worked Unrecrystallized Grains

Position	Pass 1	Pass 2
Lead End	70 pct. 150μm 30 pct. UNREX	90 pct. 210μm 10 pct UNREX
Midlength	40 pct. 80μm 60 pct. UNREX	42 pct > 160μm 28 pct. << 80μm 18 pct. 80μm 12 pct. UNREX
Tail End	100 pct. UNREX	14 pct. << 150μm 6 pct. 150μm 64 pct. 150μm 16 pct. UNREX

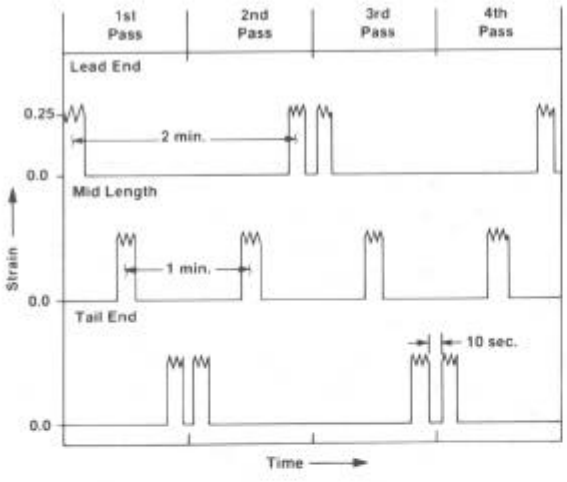

Fig. 1 - Predicted deformation-dwell time histories for three different positions along the length of a work piece processed via radial forging and for a cycle time of one minute per pass.

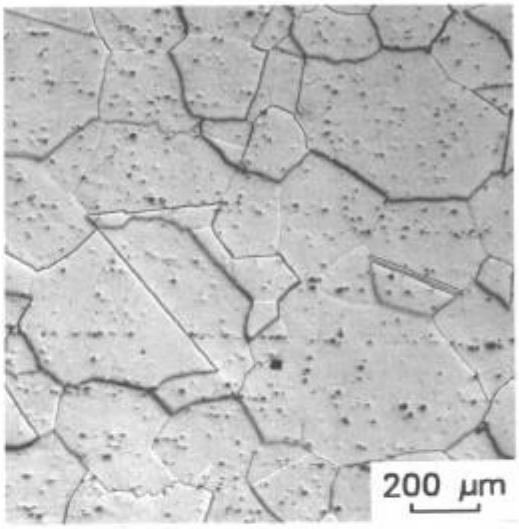

Fig. 2 - Microstructure of wrought alloy 718 after 7.5 hours at 1250°C. Starting microstructure for four-pass radial forging simulation study. Kalling's etch.

TABLE II - Composition of Alloy 718 Wrought Bar

Element	Composition in Weight Percent	Elememt	Composition in Weight Percent
C	0.044	Mg	< 0.005
Mn	0.12	B	0.0043
Si	0.21	Fe	18.99
P	0.009	Ca	< 0.010
S	0.002	Al	0.55
Cr	18.32	Ti	0.98
Mo	3.05	Sn	0.004
Cu	0.06	Pb	< 0.0005
Co	0.35	Ag	< 0.0005
Cb	5.18	Bi	< 0.5 ppm
Ta	< 0.02	Ni	Balance

TABLE III - Dwell Time in History Used to Simulate Various Work Piece Positions During Radial Forging. Dwell #1 is applied after Pass #1, etc.

Position	Dwell #1 Seconds	Dwell #2 Seconds	Dwell #3 Seconds	Dwell #4 Seconds
Lead End	130	10	130	2
Midlength	70	70	70	30
Tail End	10	130	10	60

and rolling to 16.5mm (0.65 inches) diameter bar. The bar was heat treated at 1250°C for 7.5 hours and water quenched. Hot working was applied to randomize the crystallographic texture present in the ingot, presumed to be the cause for the abnormal deformed compression sample geometry reported by Chang [1] and Weis [2], and the subsequent heat treatment coarsened the fine grained structure in the finished wrought bar to a grain size (254μm) more representative of that found in the ingot prior to breakdown. Figure 2 shows the microstructure of the wrought and heat treated material.

Compression specimens [2] for this study were taken from the wrought and heat treated bar. Four-stroke hot compression tests were performed at a constant true strain rate of $1.0s^{-1}$, at temperatures of 950°C, 1050°C, and 1150°C. The strain applied to the specimen during each stroke of an individual multiple-stroke sequence was either 0.14 or 0.23. The strain levels were chosen to simulate those typically applied during a four-pass radial forging sequence used to reduce 406mm (16 inches) diameter ingot to either 305mm (12 inches) or 254mm (10 inches) diameter billet. The hold or dwell time between strokes was varied to simulate the strain-dwell time history characteristic of either the first end of the work piece to enter the radial forge machine on the first pass (hereafter referred to as the lead end, independent of the pass number), the midlength position (midlength) or the last end of the work piece to enter on the first pass (tail end). Table III lists the strain-dwell time history for the three positions. The final dwell time for each sequence was chosen to simulate

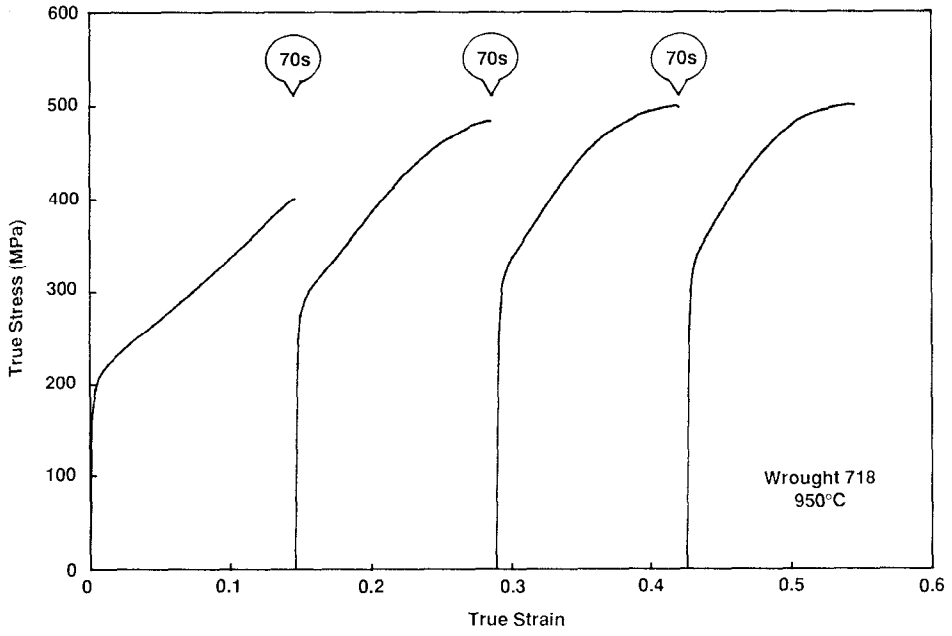

Fig. 3 - True stress-true strain curves of wrought 254μm grain diameter alloy 718 subjected to a 950°C four-pass radial forging sequence to simulate the deformation history of the midlength position of a work piece. The applied strain per pass is 0.14.

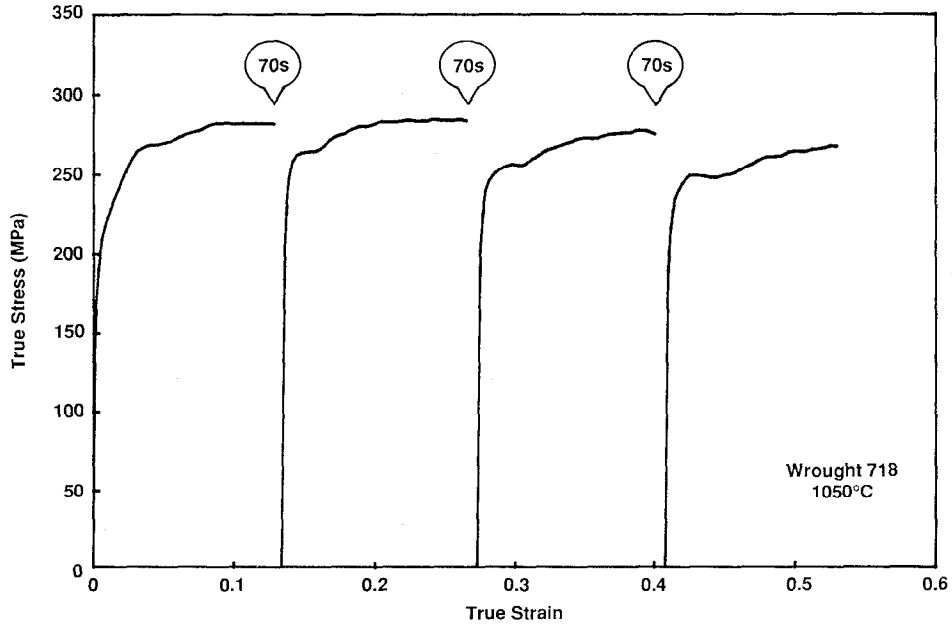

Fig. 4 - True stress-true strain curves of wrought 254μm grain diameter alloy 718 subjected to a 1050°C four-pass radial forging sequence to simulate the deformation history of the midlength position of a work piece. The applied strain per pass is 0.14.

that point at which the production work piece exists the radial forge machine for the fourth time. For example, the tail end exits the radial forge first, on the fourth pass, before the lead end exits the machine. Therefore, the test specimen simulating the tail end was held for 60 seconds (simulating one pass per minute) before quenching while the specimen simulating the lead end was rapidly quenched immediately after the fourth strain cycle was imposed.

Results and Discussion

Hot Compression Behavior

Figures 3, 4, and 5 show typical four-stroke stress-strain curves for the wrought and heat treated (254μm grain diameter) alloy 718 obtained for deformation temperatures of 950°C, 1050°C, and 1150°C, respectively. In each case the strain-dwell time history employed is typical for the midlength position of a work piece being reduced in four passes from 406mm (16 inches) to 305mm (12 inches) in diameter. Comparison of the figures shows that the maximum flow stress during multiple stroke deformation is achieved during the first stroke and is insensitive to accumulated macroscopic strain thereafter. The flow stress is however sensitive to deformation temperature, decreasing from nearly 500 MPa at 950°C to 175 MPa at 1150°C. The slight softening observed for the 950°C curves is attributed to adiabatic heating while the precipitous stress drop in the 1150°C curves is associated with the yield drop phenomenon.

Another feature of the stress-strain curves is the absence of strain softening, indicating that dynamic recrystallization is not an important grain refinement mechanism in this study. Static recrystallization, however, can and does occur during the dwell time after each strain increment. With static recrystallization, a portion of the dislocation

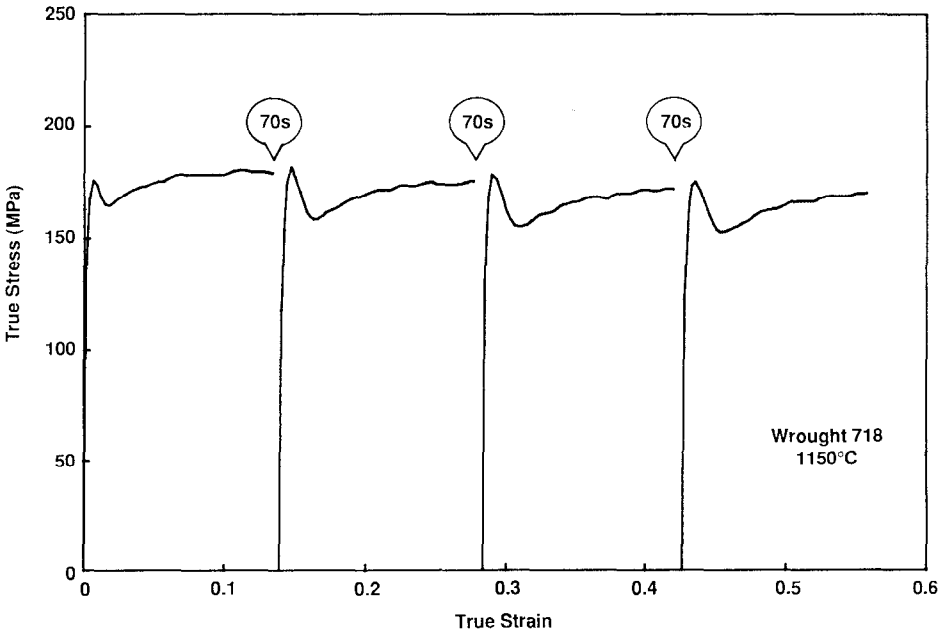

Fig. 5 - True stress-true strain curves of wrought 254μm grain diameter alloy 718 subjected to a 1150°C four-pass radial forging sequence to simulate the deformation history of the midlength position of a work piece. The applied strain per pass is 0.14.

substructure induced during the previous strain cycle is eliminated and the stress to initiate plastic deformation upon subsequent restraining is reduced. A portion of the observed softening should also be due to static recovery. At 950°C, Fig. 3, it appears that the amount of softening remains unchanged from dwell period to dwell period. However, at 1050°C, Fig. 4, the amount of softening is greater for the second and third dwell periods as compared to the first dwell period. A greater amount of softening could be attributed to an increase in static recrystallization during these latter two dwell periods.

The amount of softening that occurs during the dwell period has been calculated with the following equation:

$$S = \frac{\sigma_f - \sigma_r}{\sigma_f - \sigma_i} \cdot 100 \qquad (1)$$

where: S is the percentage of the maximum softening that could potentially be realized (maximum softening is approached as $\sigma_r \rightarrow \sigma_i$),
σ_f is the final stress prior to unloading,
σ_r is the 0.2 percent offset yield stress upon reloading after a dwell time, and
σ_i is the yield stress for the initial loading cycle.

The yield stress and softening values, for the various deformation temperatures, strain levels, work piece positions, and hold times are listed in Table IV. At 950°C, the yield stress increases from strain cycle to subsequent strain cycle indicating a general work hardening behavior, rather than softening due to either static recrystallization or static recovery. In fact, the calculated softening does not vary with strain cycle, strain level, nor with dwell time but remains constant at approximately 55 pct. Figure 6(a) shows that little recrystallization is observed after a four-stroke compression test at 950°C. All of the observed softening must then be due to static recovery. The lack of dependence of S on hold time indicates that the majority of the softening that does occur, occurs upon unloading, probably by back stress induced dislocation movement rather than by dislocation annihilation and polygonization.

At 1050°C, yield stress and softening vary dramatically with the variables studied (Table IV). For example, a four-stroke simulation of the work piece lead end with an applied strain increment per cycle of 0.14 shows that the yield stress increases from 197 MPa to 242 MPa during the first three strain cycles and then drops from 242 MPa to 217 MPa with application of the fourth strain cycle. Consistent with this variation the softening remains constant, about 50 pct. for the first two dwell periods, and then increases to 73 pct. for the third dwell period. If one assumes that approximately 50 pct. of the total softening is due to static recovery, as described above, then about half of the microstructure (23 pct. of the available remaining 50 pct.) recrystallizes statically during the third dwell period. Similarly, about half of the microstructure for the lead end, 0.23 strain/cycle specimen statically recrystallizes during the first dwell period. In fact, microstructural analysis of companion specimens quenched immediately after the first 0.23 strain increment and after 130 seconds showed that over 30 pct. of the structure recrystallizes during the dwell period. A similar test was performed for the second dwell period of the tail end, 0.23 strain/cycle. In this case 70 pct. of the structure recrystallizes statically compared to a predicted value of 68 pct. obtained from softening analysis. Evidence for extensive recrystallization at 1050°C is presented in Fig. 6(b).

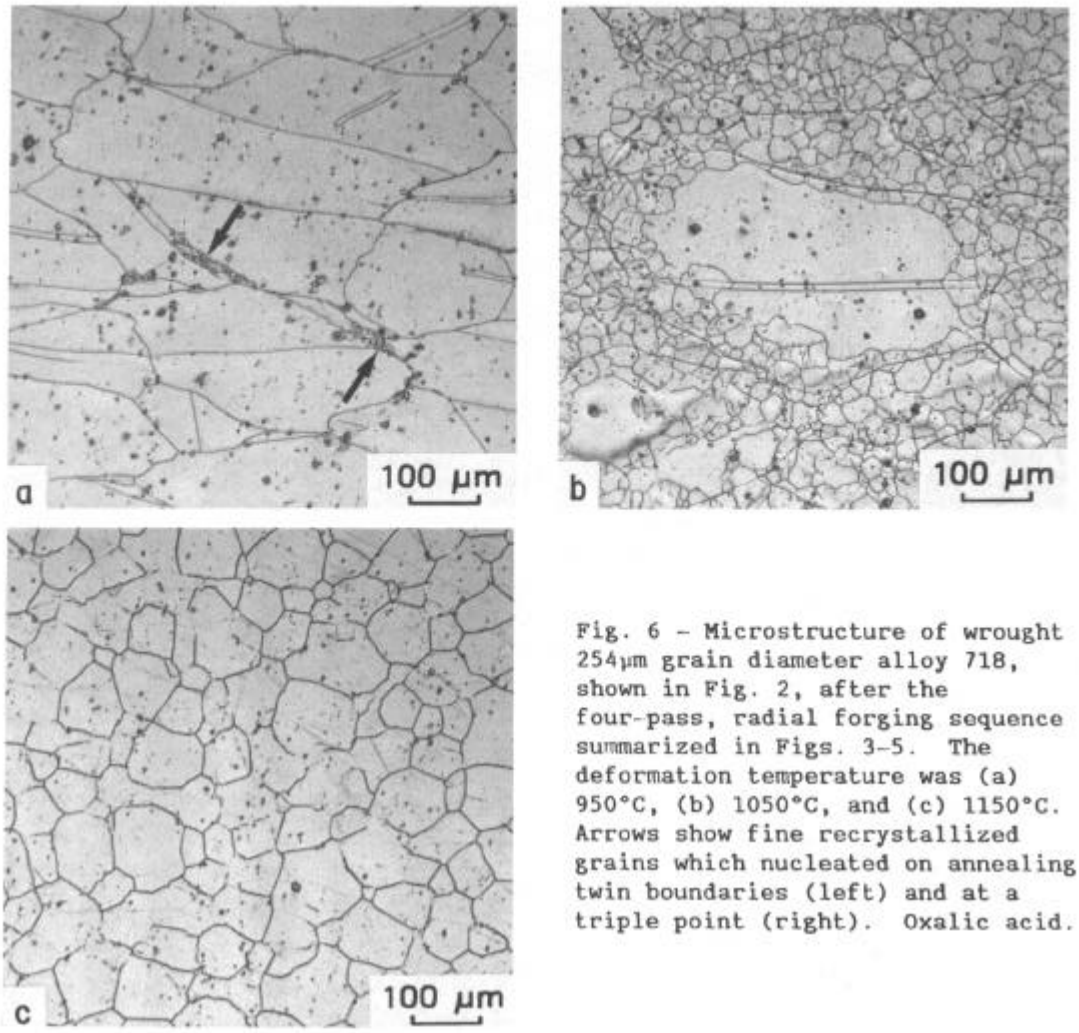

Fig. 6 - Microstructure of wrought 254μm grain diameter alloy 718, shown in Fig. 2, after the four-pass, radial forging sequence summarized in Figs. 3-5. The deformation temperature was (a) 950°C, (b) 1050°C, and (c) 1150°C. Arrows show fine recrystallized grains which nucleated on annealing twin boundaries (left) and at a triple point (right). Oxalic acid.

At 1150°C, the amount of restoration that occurs is masked by strengthening during the dwell periods as shown in Fig. 5 and Table IV. As a result softening values do not represent restoration and are not listed in Table III. Figure 6(c) showed, however, that recrystallization is a dominant restoration process at 1150°C. Strengthening may be due to short range ordering and/or solute pinning of an existing dislocation substructure. Strengthening is accompanied by a yield drop. Figures 7 and 8 show the stress-strain curves of the lead and tail ends at 1150°C. Comparison with Fig. 5 shows that strengthening and reestablishment of the yield drop progresses rapidly between 10 seconds and 70 seconds. Little further change is noted for the 70 to 130 second interval. For example, from Table IV, the yield stress for the fourth strain cycle of the 0.14 strain/cycle sequence, increases from 154 MPa to 171 MPa if the hold time is increased from 10 to 70 seconds while the yield stress for a 130 second hold is 170 MPa, equivalent to that after a 70 second hold.

Figure 9 shows the variation in yield stress with strain for the midlength, 0.14 strain/cycle sequence at 950°C and 1050°C. As discussed above, the yield stress of material deformed at 950°C increases monotonically with the application of successive strain cycles. At 1050°C, however, a critical amount of strain is reached (approximately 0.15) and upon cessation of deformation static recrystallization proceeds. A

TABLE IV - Yield Stress (0.2 pct. offset) in MPa and Percent Softening, S, for Wrought 254μm Average Grain Diameter Alloy 718 After Each Simulated Radial Forging Pass

Deformation Temperature (°C)	Position in Work Piece	Strain Per Pass	Pass 1 Yield	Pass 2 Yield (S)	Pass 3 Yield (S)	Pass 4 Yield (S)
950	Lead End	0.14	196	269 (60)	321 (54)	315 (60)
		0.23	198	294 (65)	339 (51)	322 (54)
	Midlength	0.14	196	277 (60)	306 (62)	322 (58)
		0.23	196	304 (62)	326 (56)	330 (55)
	Tail End	0.14	189	289 (51)	300 (62)	340 (52)
		0.23	196	313 (60)	317 (57)	347 (50)
1050	Lead End	0.14	197	240 (49)	242 (47)	217 (73)
		0.23	205	223 (74)	223 (72)	215 (77)
	Midlength	0.14	208	244 (51)	228 (74)	221 (82)
		0.23	201	227 (64)	216 (78)	215 (76)
	Tail End	0.14	197	250 (36)	222 (69)	225 (64)
		0.23	203	239 (51)	213 (84)	214 (80)
1150	Lead End	0.14	185	175 (--)	136 (--)	170 (--)
		0.23	174	173 (--)	151 (--)	162 (--)
	Midlength	0.14	168	173 (--)	171 (--)	171 (--)
		0.23	168	163 (--)	166 (--)	162 (--)
	Tail End	0.14	174	152 (--)	170 (--)	154 (--)
		0.23	176	148 (--)	167 (--)	153 (--)

concomitant reduction in the yield stress upon reloading occurs and is manifested in Fig. 9 as a decrease in the 1050°C curve. Also shown are the 950°C lead end, 0.23 strain/cycle and the tail end, 0.23 strain/cycle data. The apparent oscillation about the 950°C midlength curves is attributed to the alternating length of the dwell period, being either shorter or longer than the 70 second dwell characteristic of the midlength position. For example, yield stress measured after a 10 second hold is higher than the associated yield stress after a 70 second hold, and yield stress measured after a 130 second hold is lower than after a 70 second hold. This behavior is consistent for all test conditions as shown in Fig. 10. It appears then that a small portion of the static recovery at 950°C is time-dependent and is probably due to dislocation annihilation and polygonization. The majority of the static restoration however occurs very rapidly, probably on unloading. At 1050°C the time-dependent phenomena that can account for the oscillating behavior includes static recrystallization as well as static recovery.

Figure 11 shows the variation in softening (upper curves) with strain for 950°C and 1050°C. At 950°C, softening is independent of the test parameters and for the most part is time-independent. At 1050°C, softening

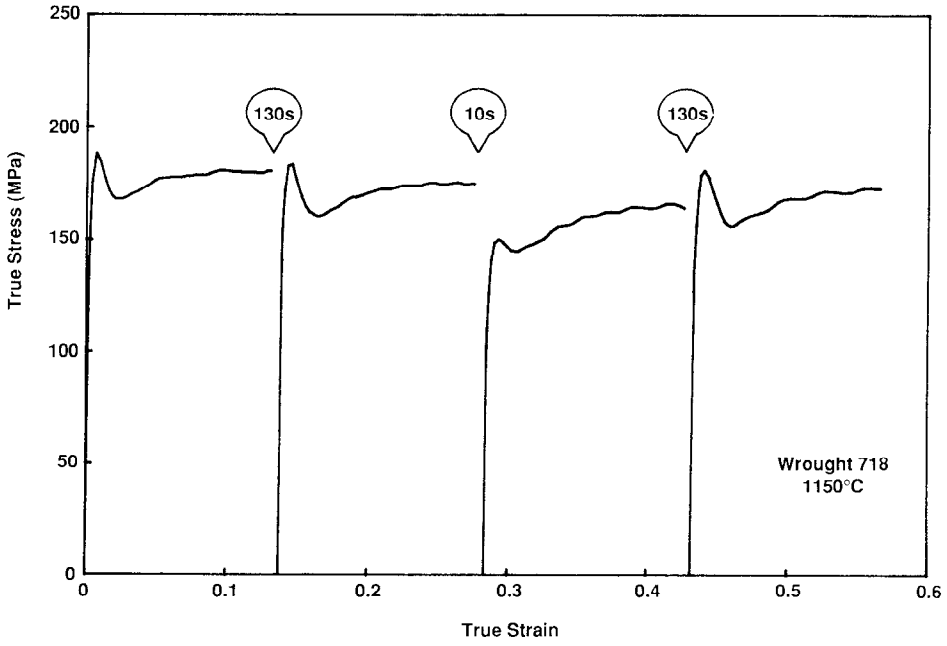

Fig. 7 - True stress-true strain curves of wrought 254μm grain diameter alloy 718 subjected to a 1150°C four-pass, 0.14 strain per pass, radial forging sequence to simulate the deformation history of the lead end position of a work piece.

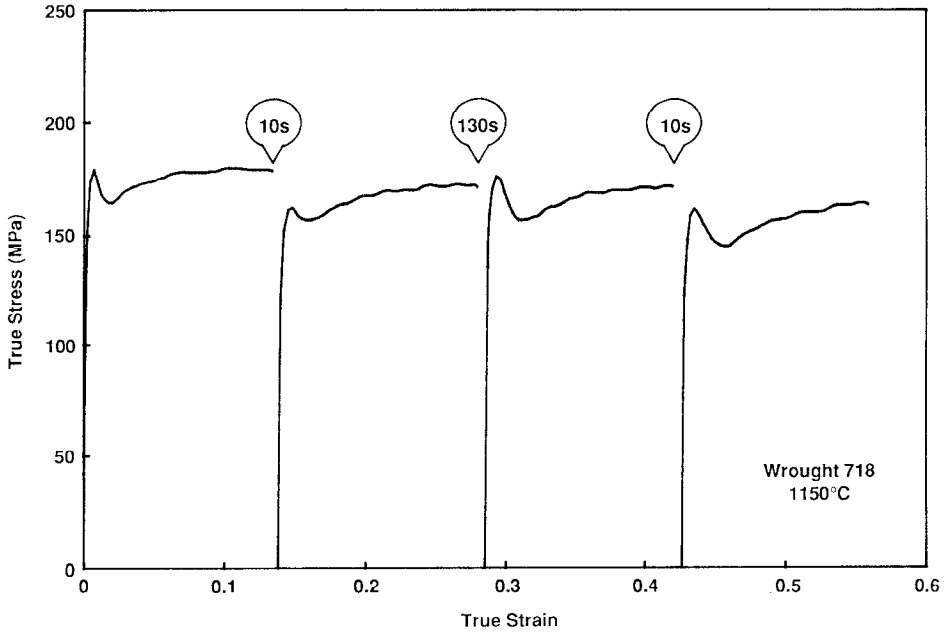

Fig. 8 - True stress-true strain curves of wrought 254μm grain diameter alloy 718 subjected to a 1150°C four-pass, 0.14 strain per pass, radial forging sequence to simulate the deformation history of the tail end position of a work piece.

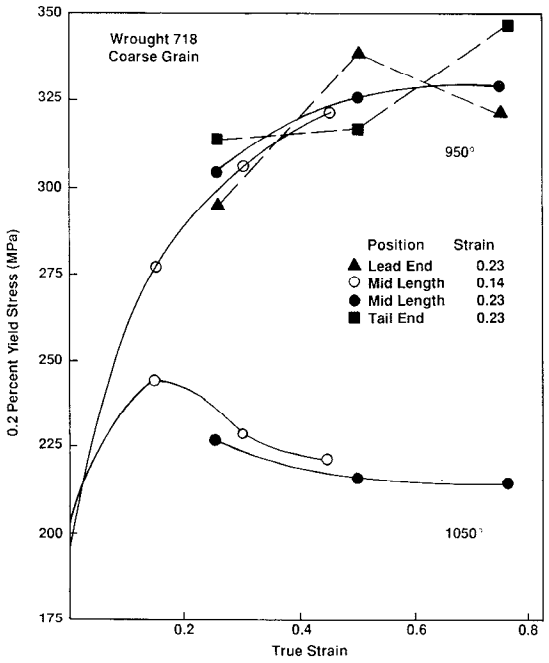

Fig. 9 - Yield stress versus total accumulated strain of wrought 254μm grain diameter alloy 718 obtained from tests simulating four-pass radial forging sequences of the midlength position. Dashed curves for the lead and tail end positions oscillate about the midlength position curve, at 950°C, showing the effect of varying dwell time between passes (see Table III for dwell times).

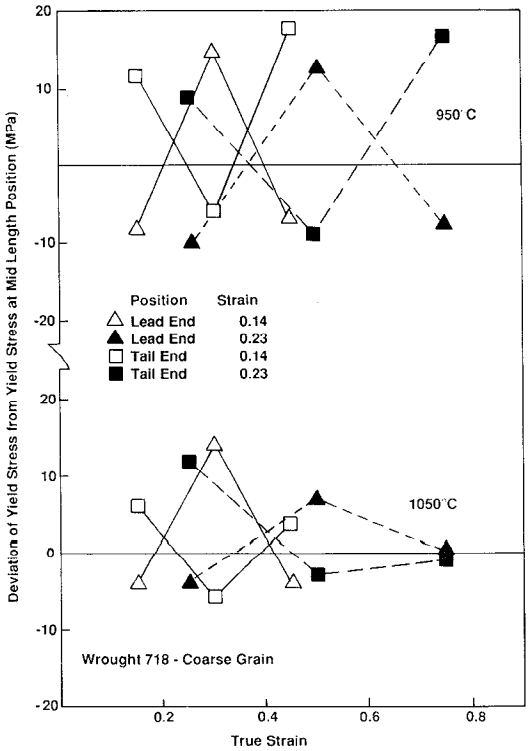

Fig. 10 - Deviation of yield stress for lead and tail end material from yield stress for midlength material as a function of total applied strain.

for the midlength material increases with accumulated strain up to a value of about 50 pct., then decreases slightly. The maximum softening recorded, approximately 75 pct., shows that as much as 50 vol. pct. of the structure can recrystallize during a 70 second dwell time. With higher applied strain (0.23 strain/cycle) as much as 70 pct. of the structure could recrystallize during a single 130 second hold.

Microstructural Evolution

Figures 12 and 13 show the evolution of the 1050°C midlength, 0.14 strain/cycle microstructure shown in Fig. 6(b) during the applied deformation-dwell time history. Immediately after applying the first strain cycle of 0.14, the specimen was rapidly quenched within two seconds. The microstructure was deformed and showed no evidence of recrystallization (micrograph not shown). Figure 12(a) shows that during the subsequent 70 second dwell period and prior to the imposition of the second strain cycle, approximately 11 pct. of the deformed microstructure statistically recrystallized. The average recrystallized grain diameter is 45μm. Figure 12(b) shows that during the following (the second) strain plus rapid quench cycle, the volume fraction recrystallized remains virtually unchanged, however, about one-half of the inherited recrystallized volume recrystallizes again. The new grains are approximately 11μm in diameter. The new grains nucleate preferentially at the initial coarse grain high angle grain boundaries, at the previously recrystallized high angle grain

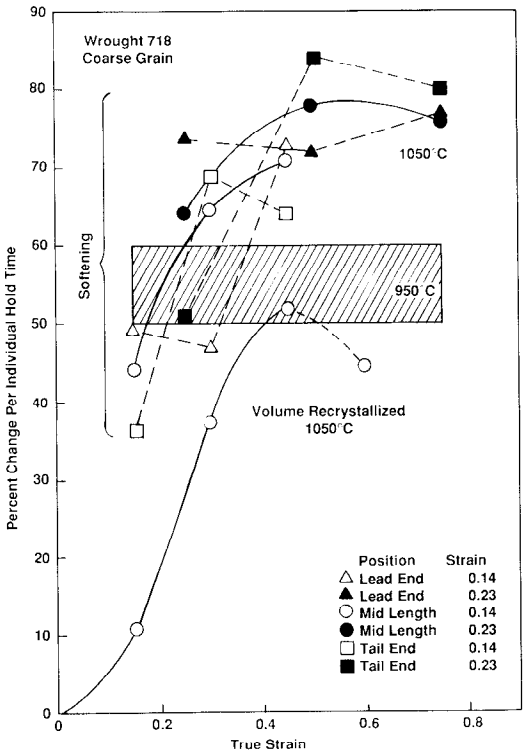

Fig. 11 - Percent softening and volume recrystallized for each individual dwell time as a function of total accumulated strain for wrought 254μm grain diameter alloy 718 subjected to four-pass radial forging simulations. Note the midlength 1050°C, 0.14 strain per pass softening curve was calculated with a σ_i of 197 MPa, a value equal to that measured for the lead and tail end samples, because the experimentally measured value in Table IV appears anamolously high.

boundaries, at the grain boundaries separating recrystallized from unrecrystallized material, and at the surface of coarse intermetallic inclusions. The second wave of recrystallization probably occurs statically after deformation and before the quench because the time for this period (1 to 2 seconds) is an order of magnitude longer than that encountered during deformation (0.15 to 0.25 seconds). This assumption is consistent with the transmission electron microscopy presented by Weis, et al. [3] for the occurrence of static recrystallization within 2 seconds after a strain of 0.25 at 1150°C, but contrary to the findings of Camus et al. [5] (refer to discussion of Fig. 8 in reference 5).

Figure 13(a) shows the microstructure corresponding to Fig. 12(b) but after a 70 second dwell time at 1050°C. A comparison of the two micrographs shows that the fine 11μm diameter grains coarsen to approximately 33μm. The remaining initially recrystallized 45μm grains coarsen to about 83μm. The structure, at this point, has a duplex grain size. The total volume fraction recrystallized increases from 11 pct. to 43 pct. with 38 pct. of the total volume being statically recrystallized during the second 70 second hold. The significant increase in volume fraction statically recrystallized, shown in Fig. 11 (lower curve), is consistent with the drop in yield stress between the second (244 MPa) and third (228 MPa) strain cycles, Table IV, and also with the large amount of softening during this hold period (74 pct.), Table IV and Fig. 11 (upper solid curve).

Figure 13(b) shows the microstructure after the third strain cycle and a rapid quench. Again, the presence of new fine recrystallized grains in coarser previously recrystallized material shows that recrystallization occurred the third time. In this case, about 30 pct. of the previously recrystallized volume recrystallized again, probably during the 2 second time period after the third strain cycle and before the quench. The new fine grains are about 17μm in diameter while the previously recrystallized grains from the prior two dwell periods have an average diameter of 75μm.

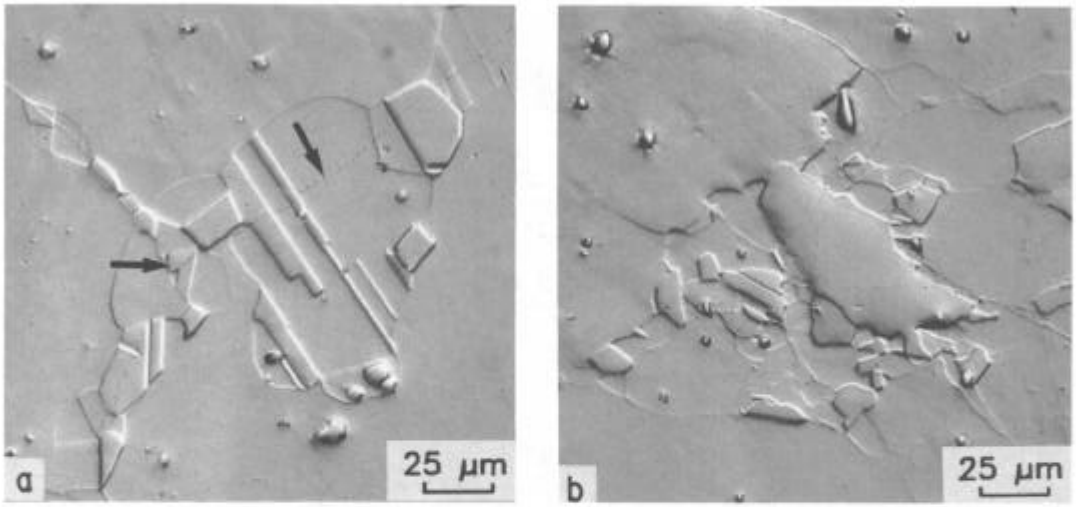

Fig. 12 - Microstructure for wrought 254μm grain diameter alloy 718 deformed at 1050°C to simulate a midlength position after (a) a strain of 0.14 (first pass) plus a 70 second hold. Note large recrystallized grain on right which nucleated at a high angle grain boundary. Arrow on right points to "ghost" appearance of prior high angle grain boundary. Arrow on left indicates location of a prior triple point; (b) a strain of 0.14 plus a 70 second dwell time plus a second strain of 0.14 (second pass) followed by a rapid (2 second) quench. Kalling's etch.

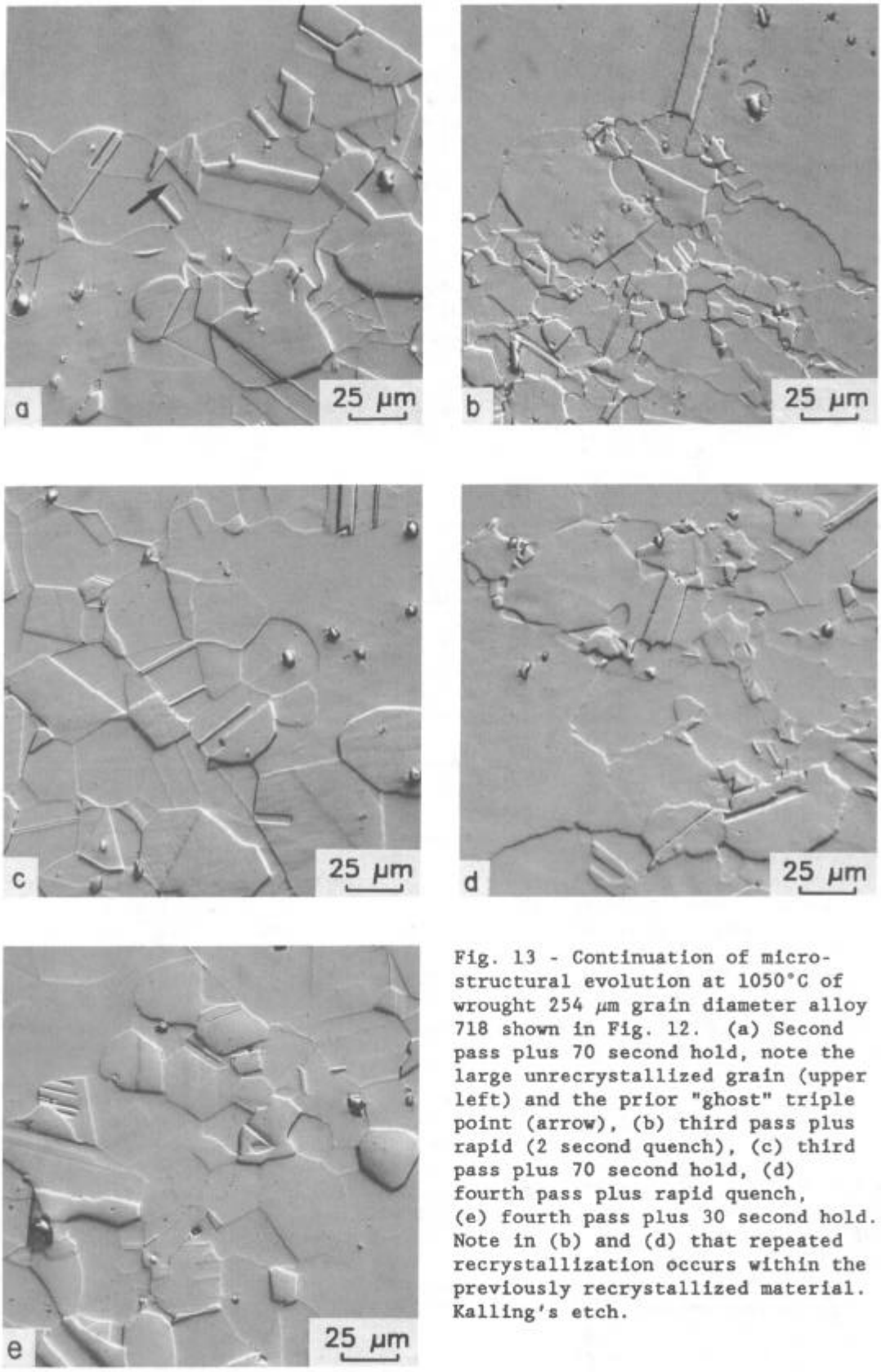

Fig. 13 - Continuation of microstructural evolution at 1050°C of wrought 254 μm grain diameter alloy 718 shown in Fig. 12. (a) Second pass plus 70 second hold, note the large unrecrystallized grain (upper left) and the prior "ghost" triple point (arrow), (b) third pass plus rapid (2 second quench), (c) third pass plus 70 second hold, (d) fourth pass plus rapid quench, (e) fourth pass plus 30 second hold. Note in (b) and (d) that repeated recrystallization occurs within the previously recrystallized material. Kalling's etch.

Figure 13(c) shows the microstructure of Fig. 13(b) after a 70 second dwell period (the third dwell applied in this sequence). During this time the 17μm grains grow to 48μm and the total volume percent recrystallized increases from 43 to 78 pct. It is estimated, from microstructural observations, that almost 50 pct. of the total volume recrystallizes statically during this hold time. Figure 13(d) shows the microstructure after the fourth strain cycle. The presence of new fine grains demonstrates that previously recrystallized material recrystallizes again, after an applied strain cycle. Figure 13(e) shows the microstructure of Fig. 13(d) after the final dwell period of 30 seconds. This is the simulated microstructure of the midlength position in a four pass radially forged billet at the 305mm (12 inches) size immediately after the final pass and prior to air cooling of the work piece. The structure is 89 pct. recrystallized with an average grain diameter of 22μm. Eleven percent of the microstructure remains unrecrystallized, Fig. 6(b), with an average grain diameter of 327μm and an occasional large unrecrystallized grain diameter, on the order of 635μm.

Table V lists the final microstructure condition, such as that described above for the 1050°C midlength, 0.14 strain/cycle sequence, for the various sequences studied. In general, deformation at 950°C is ineffective with respect to grain refinement, and the final structure obtained depends strongly on position in the work piece. For example, for strain cycles of 0.23, the tail end is 17 pct. recrystallized while the lead end is only 3 pct. recrystallized.

At 1050°C, the midlength, 0.14 strain/cycle material has a finer grain size, 22μm versus 26μm, compared to the lead end, probably due to the shorter dwell times during which grain growth is rapid. The unrecrystallized grain size is also finer due to the greater extent of recrystallization, 89 pct. versus 84 pct., respectively. Another difference associated with work piece position is that the lead end has a distinct duplex grain size and morphology with coarse grains surrounded by necklaces of fine grains. Also evident from Table V, application of a greater stain/cycle results in finer recrystallized and unrecrystallized grain sizes and a greater volume fraction recrystallized.

At 1150°C either strain level provides full recrystallization of the original coarse grain structure to a relatively fine grain microstructure, 254μm versus 60μm, respectively. Similar to the 1050°C material, a distinct duplex microstructure consisting of 25μm grain necklaces around 120μm coarse grains is found for lead end material, as shown in Figs. 14(a) and 14(b). Figures 14(c) and 14(d) show the equivalent microstructures for the midlength and tail end positions. These latter structures are much more uniform, albeit the tail end structure is slightly duplexed (but would not generally be recognized as such).

Figure 14(b), a high magnification view of Fig. 14(a), shows that the coarse recrystallized grains nucleate and grow at the prior high angle grain boundaries and triple points, while the newer fine recrystallized grains nucleate at the elder coarse recrystallized high angle grain boundaries and triple points [the "ghost" prior grain boundaries of both types are apparent in Fig. 14(b)]. The coarse grains could have originated during the first 130 second hold or during the final 130 second hold. The fact that repeated recrystallization is so prevalent at 1050°C, and that it occurs quite rapidly (within 2 seconds) gives credence for the latter scenario, coarse grains nucleating and growing during the second 130 second hold and the fine grain necklaces nucleating and growing after cessation of the fourth strain cycle and before the quench.

TABLE V - Description of Microstructure of Wrought 254mm Grain Diameter Alloy 718 Af
Simulated Radial Forging Four-Pass Sequence

Deformation Temperature (°C)	Work Piece Position	Strain Per Pass 0.14 Volume Percent Recrystallized	0.14 Average Grain Diameter (μm)	0.23 Volume Percent Recrystallized	0.23 A D
950	Lead End	UNREX		3	REX
	Midlength	< 1	REX 9	6	REX
	Tail End	2	REX 5	17	REX
1050	Lead End	84	REX Duplex(50,8) Ave Duplex 26 UNREX 507 (Max UNREX 1054)	97	REX Ave UNR (Ma
	Midlength	89	REX 22 UNREX 372 (Max UNREX 635)	96	REX UNR (Ma
	Tail End	88	REX 27 UNREX 440 (Max UNREX 635)	99	REX UNR (Ma
1150	Lead End	100	REX Duplex (120,25) Ave Duplex 56	100	REX Ave
	Midlength	100	REX 50	100	REX
	Tail End	100	REX 57	100	REX

REX = Recrystallized Grains
UNREX = Worked Unrecrystallized Grains

Comparison of Alloy 718 to Types 304L and 305 Stainless Steel

Figures 15 and 16 show typical four-stroke stress-strain curves for wrought and heat treated (1 hour at 1150°C; 250μm average grain size) type 304L stainless steel deformed at 950°C and 1150°C, respectively. Comparing these two figures to Figs. 3 and 5 shows that the flow stress of type 304L SS is about half of the stress required by alloy 718. The lack of an apparent yield drop for type 304L SS at 1150°C reinforces the earlier conclusions that the yield drop observed for alloy 718 at high temperatures is material rather than test procedure dependent. One might otherwise hypothesize that a transient from sticking to sliding friction could result in sudden drop in the flow stress and an apparent yield drop.

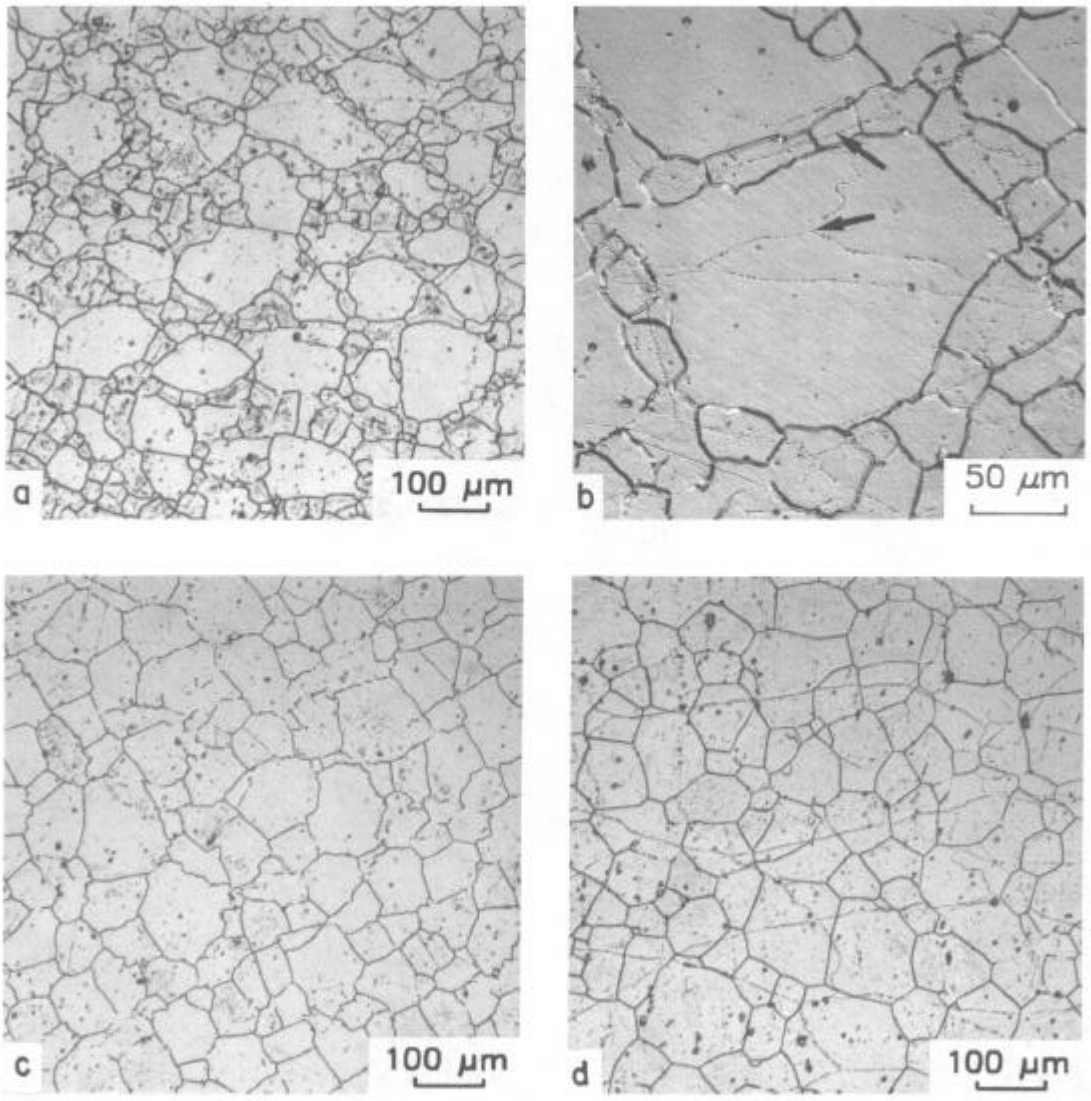

Fig. 14 - Microstructure of wrought 254μm grain diameter alloy 718 after a test simulating a four-pass radial, 0.14 strain per pass, forging sequence at 1150°C of the (a) and (b) lead end, (c) midlength position, and (d) tail end. Note the "ghost" triple point (center arrow) in (b) which was the nucleation site for a coarse grain typical of the duplex grain structure in (a), and the fine grain necklaces which nucleated on the "ghost" high angle grain boundaries (upper arrow) in (b) of the coarse grain.

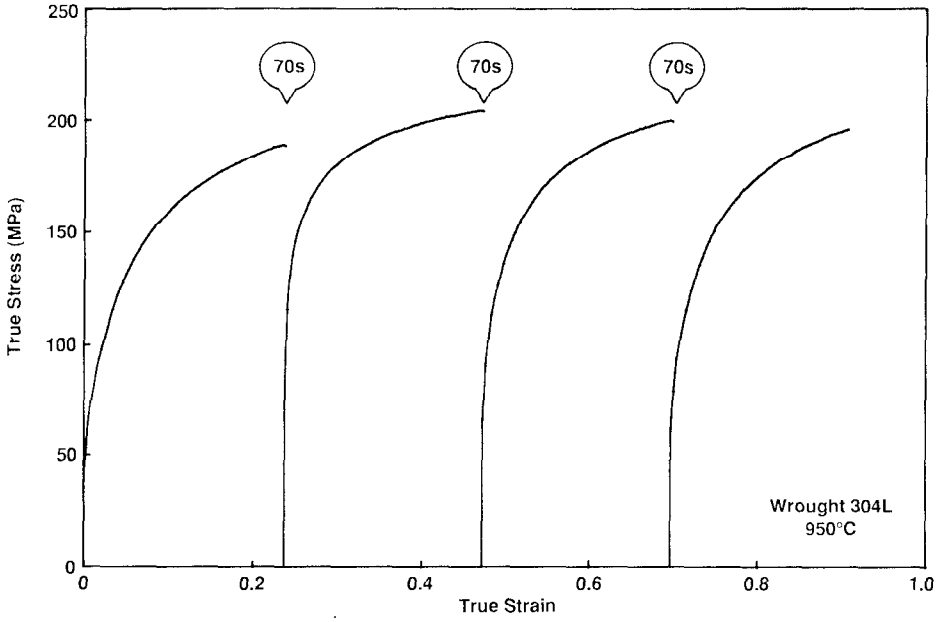

Fig. 15 – True stress-true strain curves of wrought 254μm grain diameter type 304L SS subjected to a 950°C four-pass, 0.23 strain per pass, radial forging sequence to simulate the deformation history of the midlength position of a work piece.

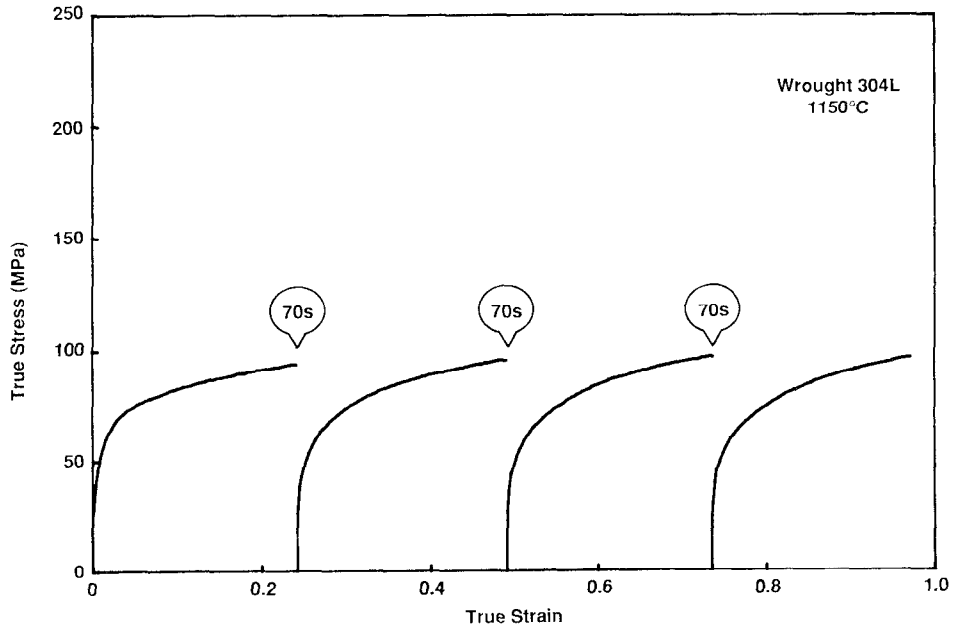

Fig. 16 – True stress-true strain curves of wrought 254μm grain diameter type 304L SS subjected to a 1150°C four-pass, 0.23 strain per pass, radial forging sequence to simulate the deformation history of the midlength position of a work piece.

TABLE VI - Yield Stress (0.2 percent offset) in MPa and Percent Softening, S, for Wrought 250μm Grain Diameter Type 304L Stainless Steel After Each Simulated Radial Forging Pass

Deformation Temperature (°C)	Position in Work Piece	Strain Per Pass	Pass 1 Yield	Pass 2 Yield (S)	Pass 3 Yield (S)	Pass 4 Yield (S)
950	Midlength	0.14	64	125 (43)	126 (52)	115 (62)
		0.23	64	123 (53)	95 (78)	84 (85)
1050	Lead End	0.14	64	52 (120)	80 (73)	52 (118)
	Midlength	0.14	64	66 (96)	54 (117)	54 (118)
		0.23	64	52 (119)	53 (118)	56 (112)
1150	Midlength	0.14	46	42 (112)	42 (111)	44 (104)
		0.23	48	36 (128)	44 (110)	43 (111)

In contrast to alloy 718, type 304L SS at 950°C recrystallizes after the second pass (note the large amount of softening in Fig. 15 between the end of the second pass and start of the third pass). The recrystallization results in significant softening and a drop in the yield stress from 123 MPa to 95 MPa as shown in Table VI. Recrystallization appears to reoccur during the third dwell period. Upon completion of the fourth pass at 950°C the midlength, 0.25 strain/cycle material is 75 pct. recrystallized as shown in Table VII, a summary of a light microscopy study. By comparison, alloy 718 is only 6 pct. recrystallized. The recrystallized grain sizes for type 304L SS are coarser than for alloy 718. As the deformation temperature is increased from 950°C to 1150°C, the apparent difference in recrystallization behavior for the two alloys (compare Tables V and VII) is moderated, and the values for volume percent recrystallized and recrystallized grain size for the two alloys approach each other. This behavior is consistent with the apparent correlation of as-cast alloy 718 to as-cast type 304L SS at high temperature [4].

Figure 17 compares the predicted grain size of the midlength of an ingot after an initial strain of 0.25 and a 70 second hold, to that observed for as-cast type 305 SS [6] for an equivalent strain and a 60 second hold. Although the approximate starting grain size of the as-cast alloy 718 is larger, the recrystallized grain sizes for the two materials after one pass at 1150°C and a one minute hold are nearly equivalent, 200μm and 160μm for type 305 SS and alloy 718, respectively. Regarding this similarity, a seemingly useful correlation of recrystallization behavior exists between alloy 718 and austenitic stainless steel. Although not plotted in Fig. 17, the final recrystallized grain size of the wrought 250μm grain diameter type 304L SS after four passes at either 950°C, 1050°C, and 1150°C, also agrees well with the as-cast type 305 SS alloy grain sizes plotted in Fig. 17. Also shown in Fig. 17 are the recrystallized grain size values measured for the wrought coarse grained alloy 718 studied here. Although the final grain size values after four passes at 1150°C are nearly equivalent for the three materials (types 305 and 304L stainless steel, and and wrought alloy 718), the recrystallized grain size is dramatically reduced for wrought alloy 718 as the deformation temperature is reduced to 950°C. The grain refinement may be associated with the presence of delta phase, Ni_3Nb, in alloy 718 which is stable to about 1040°C [1].

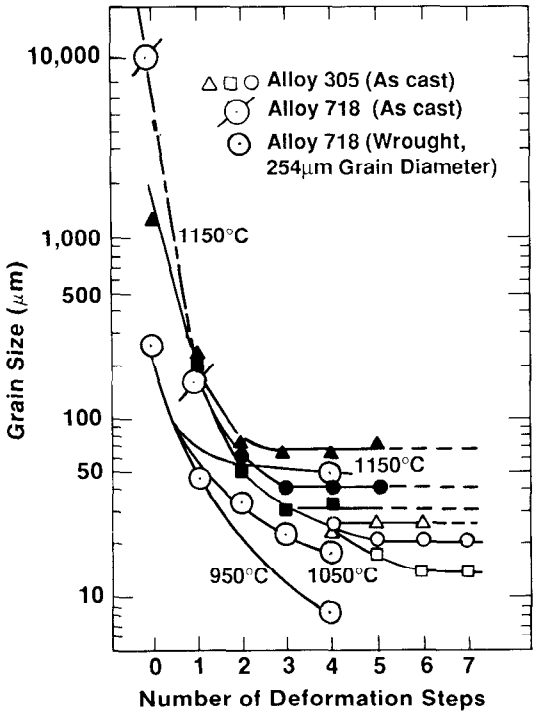

Fig. 17 - Recrystallized grain size as a function of number of deformation steps in compression for type 305 stainless steel [6] and alloy 718 (this study). Grain size for as-cast alloy 718 was calculated for a 1 min. hold after compression at 1150°C for a strain rate of $1.0s^{-1}$ and a strain of 0.25. For type 305 SS, the deformation was performed at either constant temperature, 1204°C and 1149°C, or started at 1149°C and was decreased in 55°C increments at each step until the desired finishing temperature was reached, and then held at temperature for the remaining steps. The strain rate was $10s^{-1}$. The specimen was held at temperature for one minute before the next step was applied. The data key follows:

Alloy	Symbol	Finishing Temperature (°C)	Percent Reduction
305	▲	1204	25
	●	1149	25
	■	1093	25
	Δ	1038	20
	O	982	20
	□	927	20
As-Cast 718	⌀	1150	22.2
Wrought 718	⊙	1150,1050,950	20.5

TABLE VII - Description of Microstructure of Wrought 250μm Grain Diameter Type 304L Stainless Steel After Each Simulated Radial Forging Four-Pass Sequence

		Strain Per Pass			
		0.14		0.23	
Deformation Temperature (°C)	Work Piece Position	Volume Percent Recrystallized	Average Grain Diameter (μm)	Volume Percent Recrystallized	Average Grain Diameter (μm)
950	Midlength	20	REX 27	75	REX 22
1050	Lead End	94	REX 46		
	Midlength	95	REX 43	100	REX 39
1150	Midlength	100	REX 66	100	REX 52

REX = Recrystallized Grains

Figure 17 for type 305 SS indicates that the finish temperature determines the final grain size. Roberts, et. al. [7], investigating two austenitic stainless steels, showed that the rate of dynamic recrystallization varied inversely with initial grain size, D_o, and that at a given temperature and strain rate, the critical strain for dynamic recrystallization decreased significantly as D_o decreased. Thus, as the coarse ingot grain structure is reduced via static recrystallization during the dwell times between the initial passes, the critical strain for dynamic recrystallization would also be reduced. Guimaraes and Jonas [8] observed full dynamic recrystallization in alloy 718 after a strain of 0.7 at 1090°C. Although not cited, the initial grain size was apparently about 150μm, similar to that predicted for alloy 718 ingot after two passes (Table II). If dynamic recrystallization occurs during later passes it would be favored at the midlength by the finer grain size and at the bar ends because of the short ten second dwell time which results in greater cumulative strain to drive dynamic recrystallization. Dynamic recrystallization would not be expected to occur fully on the 3rd or 4th passes when considering the data of Guimaraes and Jonas. Static recrystallization remains the dominant grain refinement mechanism as shown here by the sequence of microstructures in Fig. 13 for 1050°C multiple stroke compression. In fact, significant softening of the flow curves which would be indicative of dynamic recrystallization was never observed.

Microstructural Development in Gradients

In the modeling of microstructural evolution during breakdown, a number of other effects need to be considered. For example, in heavy forging the work does not penetrate efficiently from surface to center in the work piece. If the center of an ingot receives less strain than the surface during working, then grain refinement at the center should lag the surface. In fact, in their study of the deformation of as-cast copper, Matlock and Burford [9] showed that the gradient in strain from surface to centerline of the ingot, created by varying the deformation zone geometry (Δ), resulted in a distinct and steep gradient in structure during subsequent annealing.

The surface was fully recrystallized while the center was unrecrystallized for Δ greater than four where Δ is measured by dividing work piece through-thickness by die contact length. As the alloy 718 bar is processed to a smaller diameter, Δ decreases and the ingot center would be worked more effectively.

Gradients in redundant work [9] should result in temperature gradients due to adiabatic heating. In this case the surface should be cooler than the center due to heat loss to the environment but preferential adiabatic heating of the surface would lessen the temperature gradient from surface to center. The work applied at lower temperature is more effectively retained because of reduced dynamic recovery and is available to drive static recrystallization at a more rapid rate at the surface as temperature subsequently increases due to adiabatic heating.

Both cooler surface temperatures and the varying solidification texture are associated with reduction in the flow stress from surface to center. Although the resultant gradient in flow stress could be significant, as great as a 50 pct decrease from surface to center during reduction, the overall effect on the penetration of work and the recrystallization kinetics are complex and remain unexplained at this point.

Conclusions

1. In alloy 718 static recrystallization is the principle grain refinement mechanism for the initial part of ingot breakdown by radial forging. At the applied strains and temperatures, the deformation temperature and time between deformation cycles are the primary production variables which are predicted to control structural evolution.

2. Anticipated variations in the dwell time sequence for different positions along the length of a radial forging work piece should result in microstructural variations along the work piece. For example, after multiple-pass deformation at 1150°C, the lead end should have a distinctly different (a duplex grain size) microstructure compared to the other positions in the work piece which have a relatively uniform grain size.

3. In the four-pass radial forging simulations, complete recrystallization of the initially coarse grain structure occurred only at the highest temperature studied (1150°C). The average grain size throughout the finished simulated work piece was acceptable, 60μm in diameter (ASTM 5.0), however, grains as large as 120μm in diameter (ASTM 3.0) were characteristic of the duplex microstructure in the lead end of the work piece. Grain coarsening would be expected during the cool down period after forging.

4. Recrystallization of previously recrystallized material occurs repeatedly with the imposition of strain-dwell cycles subsequent to the cycle that first induced recrystallization. Repeated recrystallization is a major contributor in the maintenance of a fine grain microstructure during multiple-pass forging sequences at high temperatures.

5. The amount of softening, calculated from the stress-strain behavior of multiple-stroke compression tests, is useful in estimating the degree of static recrystallization in alloy 718. Unfortunately, strengthening during dwell periods at 1150°C masks the effect, and the calculated softening is not indicative of static restoration alone.

6. Grain size refinement in alloy 718 during multiple-pass forging sequences applied at 1150°C appears to be similar to that found for stainless steel alloys 304L and 305. However, at lower forging temperatures little similarity exists.

7. Other variables which may be important to the evolution of the microstructure during primary breakdown do exist but their effect has not been quantified here. Some are the deformation zone geometry, temperature fluctuations from atmospheric loss or adiabatic gain, and gradients in redundant work from variations in solidification texture.

ACKNOWLEDGMENTS

The authors acknowledge the support of the Advanced Steel Processing and Products Research Center, a National Science Foundation supported cooperative research center, at the Colorado School of Mines, and Michael P. Riendeau for his engineering support of the multiple stroke compression testing. The authors also acknowledge the assistance of Dr. M. L. Robinson of the Carpenter Technology Corporation. Sincere thanks are given to Ms. Nina Eads for typing this manuscript.

REFERENCES

1. D. A. K. C. Chang, "The Influence of Ingot Heterogeneity Upon the Hot Deformation of Alloy 718", M.S. Thesis No. T-3371, Colorado School of Mines, Golden, Colorado (1987).
2. M. J. Weis, "The Hot Deformation Behavior of As-Cast Alloy 718", M.S. Thesis No. T-3382, Colorado School of Mines, Golden, Colorado (1987).
3. M. J. Weis, M. C. Mataya, S. W. Thompson, and D. K. Matlock, "The Hot Deformation Behavior of an As-Cast Alloy 718 Ingot", in Alloy 718-Metallurgy and Applications, TMS, Warrendale, Pennsylania, 1989 (proceedings from International Symposium on Alloy 718, Pittsburgh, Pennsylvania, 1989, this publication).
4. M. C. Mataya, M. L. Robinson, D. Chang, M. J. Weis, G. R. Edwards, and D. K. Matlock, "Grain Refinement During Primary Breakdown of Alloy 718", 29th Mechanical Working and Steel Processing Conference Proceedings, ISS of AIME, Toronto, Ontario, Canada, vol. XXV, pp. 235-248 (1987).
5. G. Camus, B. Pieraggi, and F. Chevet, "Hot Deformation and Recrystallization of Inconel 718", Formability and Metallurgical Structure, Edited by A. K. Sachdev and J. D. Embury, TMS, Inc., Warrendale, Pennsylvania, pp. 305-324 (1986).
6. M. R. Staker and N. J. Grant, "The Effects of Strain, Strain Rate, and Temperature on Grain Refinement and Hot Workability of Type 305 Stainless Steel", Mater. Sci. Engr., vol. 75, pp. 137-150 (1985).
7. W. Roberts, H. Boden, and B. Ahlblom, "Dynamic Recrystallization Kinetics", Met. Sci., vol. 13, pp. 195-205, March-April (1979).
8. A. A. Guimaraes and J. J. Jonas, "Recrystallization and Aging Effects Associated with the High Temperature Deformation of Waspaloy and Inconel 718", Metall. Trans. A, vol. 12A, pp. 1655-1666, September (1981).
9. D. K. Matlock and D. A. Burford, "An Experimental Correlation of Plane Strain Deformation Zone Geometry and Forming Loads", Journal of Applied Metalworking, vol. 4, no. 4, pp. 301-305, January (1987).